

Robust Control of a Platoon of Underwater Autonomous Vehicles

A. Okamoto, J. J. Feeley, D. B. Edwards, R. W. Wall

Center for Intelligent Systems Research

University of Idaho

Moscow, Idaho, 83843-0902, U.S.A

E-Mail: okam2217@uidaho.edu

Abstract - Effective control systems for a variety of underwater autonomous vehicles have been developed and are in use. These systems generally assume the vehicle is operating independently of other nearby vehicles. However, there is recent and growing interest in the coordinated control of a platoon of vehicles acting cooperatively to achieve an objective that a single vehicle operating alone cannot achieve.

This paper presents the design of a robust multivariable controller for decentralized leader-follower control of a platoon of autonomous underwater vehicles. A three degree-of-freedom model of the REMUS underwater vehicle is used as an example case for control in a plane. The design is based on Linear Quadratic Gaussian Regulator theory with Loop Transfer Recovery. A way point guidance system is used for lead vehicle navigation. Follower vehicles maintain specified range and bearing to adjacent vehicles.

The resulting control system is used in a computer simulated search for randomly distributed mines. A three vehicle fleet is used to demonstrate superiority, in terms of area coverage and elapsed time, over a single vehicle search. Simulations are performed both with and without ocean current disturbances. A unique formation swap maneuver is introduced to make an efficient 180 degree turn in a mow-the-lawn type multi-vehicle search.

I. INTRODUCTION

Even though various kinds of autonomous vehicles have been designed and constructed, they usually operate individually or independently with others. Recently, interest in a coordinated or cooperative control scheme for a platoon of autonomous vehicles has grown. The general idea is to use relatively inexpensive, simple, and small vehicles to cooperatively solve a difficult problem. For example, Mataric et al used two autonomous six-legged robots to cooperatively push a box [12]. Kang et al designed a formation controller for multiple micro satellites for synthetic-aperture imaging [8].

Potential applications for a platoon of autonomous underwater vehicles (AUVs) are minesweeping and ocean floor survey. For example, a formation of AUVs and a master AUV can be used to form a multi-static synthetic aperture [3]. Healey introduced supervisor/swimmer control

logic for a platoon of AUVs for minesweeping [6]. In his algorithm, each vehicle follows predefined search tracks. If any of the vehicles are lost, the supervisor commands the remaining vehicles to shift their search tracks to fill in the gap. Kuroda et al designed a multi-vehicle random search algorithm, which consists of simple individual and cooperative behaviors, to search for scattered targets [9].

In this paper, we introduce a robust leader-follower control algorithm and perform one of the popular multi-vehicle search methods, a "mow the lawn" search, where vehicles fly in formation and sweep predefined search lanes. We assume that the leader knows its inertial position and the followers only know a range and a bearing to the leader. The leader navigates using a waypoint guidance system. The followers maintain specified distances to the leader. The formation shape is determined by considering a search pattern and capacity of detecting sensors to minimize search time and maximize probability of detection. We introduce a formation swap maneuver in which the vehicles swap their formation position with virtual followers to achieve an efficient 180deg turn. Simulations are done with and without ocean current disturbances. The performance of the multi-vehicle search is compared with that of single vehicle search.

The controller for both the leader and the followers are designed based on Linear Quadratic Gaussian regulator (LQG) theory and Loop Transfer Recovery (LTR). The LQG controller consists of a Linear Quadratic Regulator (LQR) and a Kalman filter. Although it is well known that the LQR controller has good robustness properties, these properties are usually lost when the controller is used in conjunction with the Kalman filter [1]. Hence, the LTR technique given in [2] is often applied to recover robustness of the overall LQG system.

Previously, LQG/LTR design method has been used for submersibles. Martin et al designed a LQG/LTR controller with an active roll controller to reduce unwanted depth changes [11]. Juul designed a gain-scheduled LQG/LTR controller for four different operating speeds [7]. Naeem designed a hybrid guidance controller in which vehicle speed control was included as part of a navigation system for underwater cable following problem [13]. In this paper, we design an LQR/LTR controller to control the formation of a platoon of autonomous underwater vehicles.

Report Documentation Page			Form Approved OMB No. 0704-0188		
Public reporting burden for the collection of information is estimated to average 1 hour per response, including the time for reviewing instructions, searching existing data sources, gathering and maintaining the data needed, and completing and reviewing the collection of information. Send comments regarding this burden estimate or any other aspect of this collection of information, including suggestions for reducing this burden, to Washington Headquarters Services, Directorate for Information Operations and Reports, 1215 Jefferson Davis Highway, Suite 1204, Arlington VA 22202-4302. Respondents should be aware that notwithstanding any other provision of law, no person shall be subject to a penalty for failing to comply with a collection of information if it does not display a currently valid OMB control number.					
1. REPORT DATE 2004		2. REPORT TYPE		3. DATES COVERED 00-00-2004 to 00-00-2004	
4. TITLE AND SUBTITLE Robust Control of a Platoon of Underwater Autonomous Vehicles			5a. CONTRACT NUMBER		
			5b. GRANT NUMBER		
			5c. PROGRAM ELEMENT NUMBER		
6. AUTHOR(S)			5d. PROJECT NUMBER		
			5e. TASK NUMBER		
			5f. WORK UNIT NUMBER		
7. PERFORMING ORGANIZATION NAME(S) AND ADDRESS(ES) University of Idaho,Center for Intelligent Systems Research,Moscow,ID,83844			8. PERFORMING ORGANIZATION REPORT NUMBER		
9. SPONSORING/MONITORING AGENCY NAME(S) AND ADDRESS(ES)			10. SPONSOR/MONITOR'S ACRONYM(S)		
			11. SPONSOR/MONITOR'S REPORT NUMBER(S)		
12. DISTRIBUTION/AVAILABILITY STATEMENT Approved for public release; distribution unlimited					
13. SUPPLEMENTARY NOTES The original document contains color images.					
14. ABSTRACT					
15. SUBJECT TERMS					
16. SECURITY CLASSIFICATION OF:			17. LIMITATION OF ABSTRACT	18. NUMBER OF PAGES 6	19a. NAME OF RESPONSIBLE PERSON
a. REPORT unclassified	b. ABSTRACT unclassified	c. THIS PAGE unclassified			

II. THE 3DOF REMUS MODEL

REMUS (Remote Environmental Measuring UnitS) is a low-cost autonomous underwater vehicle, originally developed by Woods Hole Oceanographic Institute. The six degree-of-freedom (DOF) model of REMUS is developed and verified in [15], and we use it as an example case to demonstrate effectiveness of our control system. We use the same model for both a leader and followers.

The six DOF model is reduced to a three-degree-of-freedom model to study the vehicle's motion in the horizontal plane. The plant's states will be forward velocity, u , lateral velocity, v , and yaw rate, r , and inputs will be the propeller thrust, u_{prop} , and the rudder angle, δ_r . The linear model is found as:

$$\begin{aligned} \dot{x} &= Ax + Bu_{in} \\ y &= Cx + Du_{in} \end{aligned} \quad (2.1)$$

where $x = [u \ v \ r \ \psi]^T$, $u_{in} = [u_{prop} \ \delta_r]^T$ and

$$A = \begin{bmatrix} -0.372 & 0 & 0 & 0 \\ 0 & -2.7815 & -0.6315 & 0 \\ 0 & -5.0016 & -1.9732 & 0 \\ 0 & 0 & 1 & 0 \end{bmatrix}$$

$$B = \begin{bmatrix} 0.0032 & 0 \\ 0 & 0.2821 \\ 0 & -1.5952 \\ 0 & 0 \end{bmatrix}$$

$$C = \begin{bmatrix} 1 & 0 & 0 & 0 \\ 0 & 0 & 0 & 1 \end{bmatrix}$$

$$D = 0$$

where

u is a forward velocity in *m/sec*

v is a lateral velocity in *m/sec*

r is yaw rate in *rad/sec*

ψ is yaw angle in *rad*

Inputs are

u_{prop} is a propeller thrust in *N*

δ_r is a rudder angle in *rad*

Its operating point was chosen as $x_o = [1.5 \ 0 \ 0 \ 0]$ and $u_{in,o} = [8.718 \ 0]$. Note that the equation for yaw is added to the original three-DOF model. It was assumed that the outputs are forward velocity and yaw.

Since (2.1) is defined in a body-fixed (local) coordinates, the following equation is required to find the vehicle's inertial position.

$$\begin{aligned} \dot{X} &= u \cos \psi + v \sin \psi \\ \dot{Y} &= -u \sin \psi + v \cos \psi \end{aligned} \quad (2.2)$$

Where X and Y are inertial coordinates and the variables for this 3DOF model are graphically illustrated in Fig. 1.

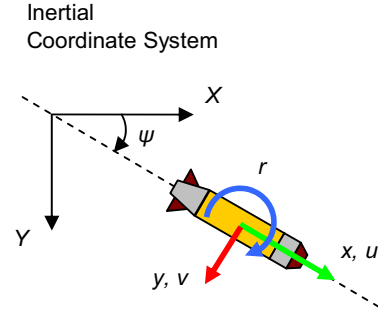


Fig. 1 : Local and Inertial Coordinate Systems

III. CONTROLLER DESIGN FOR A LEADER AND FOLLOWERS

The controller consists of two subsystems: a steering controller and a speed controller. Both the leader and followers use the same steering controller; it tries to look at a desired point. The desired point is a waypoint for the leader and a desired formation position for the followers. Fig. 2 shows the variables required for formation control. X and Y represent inertial coordinates, and we use x_i and y_i to represent the i^{th} vehicle's body-fixed coordinates. The leader is vehicle 0 and the i^{th} follower is vehicle i . In designing the controllers, we assume that all followers are able to measure a range and a bearing to the leader. We also assume that there is no delay on the measurements, and the measurements are continuous.

The steering controller tries to set a heading to a desired heading (ψ_{di}). This can also be done by minimizing a line-of-sight angle ($\theta_{LOS,i}$) and it is determined as:

$$\begin{aligned} \theta_{LOS,i} &= \psi_{di} - \psi_i \\ \psi_{di} &= \tan^{-1} \left(\frac{Y'_{di} - Y'_i}{X'_{di} - X'_i} \right) \end{aligned} \quad (3.1)$$

where (X'_{di}, Y'_{di}) is a waypoint or a desired formation position for vehicle i , and (X'_i, Y'_i) is the i^{th} vehicle's absolute position. From (3.1) we see that either absolute positions or relative positions are required for the steering control. However, we need to be careful about two things. First, in order for the leader to navigate smoothly with the waypoints, a circle of acceptance needs to be provided [4, 5]. We set the radius of the circle to be the leader's turning radius for an optimal 90deg turn. Second, the line-of-sight angle becomes sensitive to noise when a follower converges to its desired position. Hence, we need to design a speed controller such that the followers always chase the point.

The leader's speed controller regulates the velocity at the operating velocity while the followers' controller adjusts a velocity to minimize a forward distance ($e_{x,i}$) to the desired formation position. Notice that the forward distance is different from a range. The forward distance is defined as

$$e_{x,i} = x'_0 - x'_i - x'_{d0i} - k \quad (3.2)$$

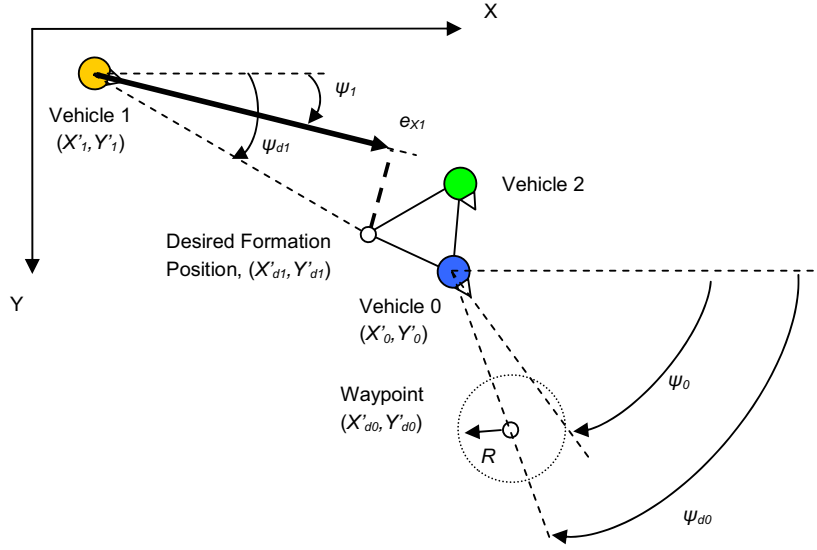


Fig. 2 : Variables for Navigation and Formation Control

where x'_i is the i^{th} vehicle's position and x'_{d0i} is a desired vehicle separation in x_r -direction. We added a constant, k , to (3.2) so that the followers always chase the point. Derivative of (3.2) yields

$$\dot{e}_{x,i} = \dot{x}'_0 - \dot{x}'_i - \dot{x}'_{d0i} - \dot{k} = u_0 - u_i \quad (3.3)$$

where u_i is a forward velocity of vehicle i , u_0 a forward velocity of the leader. All of these variables are in the i^{th} follower's local coordinates.

Introducing (3.2) as a new state and augmenting (3.3) to (2.1) yields a state equation for a follower:

$$\begin{bmatrix} \dot{u}_i \\ \dot{v}_i \\ \dot{r}_i \\ \dot{\psi}_i \\ \dot{e}_{x,i} \end{bmatrix} = \begin{bmatrix} -0.372 & 0 & 0 & 0 & 0 \\ 0 & -2.7815 & -0.6315 & 0 & 0 \\ 0 & -5.0016 & -1.9732 & 0 & 0 \\ 0 & 0 & 1 & 0 & 0 \\ -1 & 0 & 0 & 0 & 0 \end{bmatrix} \begin{bmatrix} u_i \\ v_i \\ r_i \\ \psi_i \\ e_{x,i} \end{bmatrix} + \begin{bmatrix} 0.032 & 0 \\ 0 & 0.2831 \\ 0 & -1.5952 \\ 0 & 0 \\ 0 & 0 \end{bmatrix} \begin{bmatrix} u_{prop,i} \\ \delta_{r,i} \end{bmatrix} + \begin{bmatrix} 0 \\ 0 \\ 0 \\ 0 \\ 1 \end{bmatrix} u_0 \quad (3.4)$$

Assuming that the follower knows the distance to the leader, the output equation is determined as:

$$y_i = \begin{bmatrix} 1 & 0 & 0 & 0 & 0 \\ 0 & 0 & 0 & 1 & 0 \\ 0 & 0 & 0 & 0 & 1 \end{bmatrix} \begin{bmatrix} u_i \\ v_i \\ r_i \\ \psi_i \\ e_{x,i} \end{bmatrix} \quad (3.5)$$

For the leader, we use an integral of velocity error,

$$e_{x,0} = \int (u_{ref} - u_0) dt \quad (3.6)$$

in stead of (3.2). Then, the leader's equation becomes

$$\begin{bmatrix} \dot{u}_0 \\ \dot{v}_0 \\ \dot{r}_0 \\ \dot{\psi}_0 \\ \dot{e}_{x,0} \end{bmatrix} = \begin{bmatrix} -0.372 & 0 & 0 & 0 & 0 \\ 0 & -2.7815 & -0.6315 & 0 & 0 \\ 0 & -5.0016 & -1.9732 & 0 & 0 \\ 0 & 0 & 1 & 0 & 0 \\ -1 & 0 & 0 & 0 & 0 \end{bmatrix} \begin{bmatrix} u_0 \\ v_0 \\ r_0 \\ \psi_0 \\ e_{x,0} \end{bmatrix} + \begin{bmatrix} 0.032 & 0 \\ 0 & 0.2831 \\ 0 & -1.5952 \\ 0 & 0 \\ 0 & 0 \end{bmatrix} \begin{bmatrix} u_{prop,0} \\ \delta_{r,0} \end{bmatrix} + \begin{bmatrix} 0 \\ 0 \\ 0 \\ 0 \\ 1 \end{bmatrix} u_{ref} \quad (3.7)$$

$$y_0 = \begin{bmatrix} 1 & 0 & 0 & 0 & 0 \\ 0 & 0 & 0 & 1 & 0 \\ 0 & 0 & 0 & 0 & 1 \end{bmatrix} \begin{bmatrix} u_0 \\ v_0 \\ r_0 \\ \psi_0 \\ e_{x,0} \end{bmatrix} \quad (3.8)$$

which is almost identical to (3.4). Note that $e_{x,0}$ and $e_{x,i}$ have different meaning; $e_{x,0}$ is an integral of velocity error while $e_{x,i}$ is a distance to the desired formation position.

A Linear Quadratic Gaussian (LQG) controller was designed for the system given in (3.4) and (3.7). Then, the Loop Transfer Recovery (LTR) technique was used to recover robustness [1, 2, 10]. The LTR method works on the plant if it is controllable, observable, and minimum phase [1]. For the plants with more outputs than inputs, LTR is possible at the plant input by adding a dummy column to the system B matrix and a zero row to the LQR controller gain matrix [1, 2]. Hence we added a dummy column to the second term in the right hand side of (3.4) and (3.7) and a zero row to their LQR controller gain matrices. We first designed a LQR controller and used it as our target feedback loop (TFL). Then the Kalman filter was adjusted to recover the robustness of the overall system.

The singular value plot of the leader and the follower is given in Fig. 3a and Fig. 3b. The dashed lines are a maximum and a minimum singular value plot of the target feedback loop (TFL), and solid lines are that of recovered system. When calculating the LQR controller gains, penalties for the states were carefully chosen to minimize the formation errors and the deviation in heading in order to keep the vehicles steady. Also, the penalties were chosen to avoid actuator saturation as much as possible.

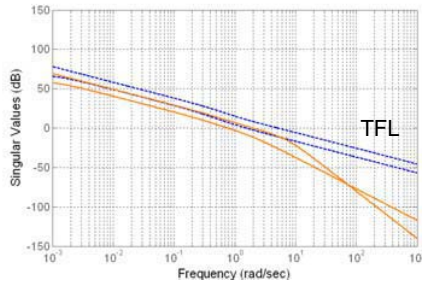


Fig. 3a: Singular Value Plots of Leader's Target Feedback Loop (TFL) and LQG/LTR

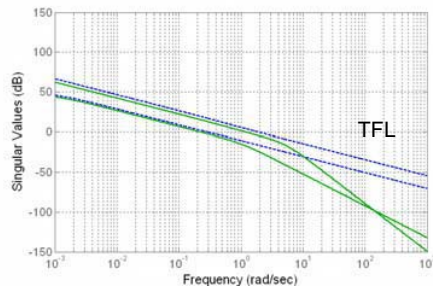


Fig. 3b: Singular Value Plots of Followers' Target Feedback Loop (TFL) and LQG/LTR

IV. FORMATION SWAP MANEUVER

In this section, we introduce a formation swap maneuver where a formation is swapped at every 180deg turn to make an efficient turn. When a formation shape is defined with respect to the leader, it rotates as the leader rotates which results a very inefficient turn. Here, we define our formation shape in the fixed coordinate system as well as a follower's local coordinate system. In this way, the formation is changed at every corner without any extra communication.

For the formation swap, the asymmetric formation given in Fig. 4 is used. It allows the followers to make a smooth formation change because the directions of a turn and a swap are the same as for a lawn-mower search. Notice that the lateral distance between each vehicle is defined in the fixed coordinates while the forward distance is defined in the local coordinates.

In Fig. 5, the dotted lines are trajectories of five vehicles when the same formation is maintained during the turn. Note that the shaded vehicles are virtual vehicles and do not physically exist. From the figure, we see that vehicles have to increase or decrease their velocity during the turn depending on their formation position. This will become more and more serious as a platoon gets larger and larger. With the formation change, the real followers change their

trajectories with the virtual followers as shown in the figure. Use of the virtual followers avoids potential collisions during the process. When the leader arrives at the first waypoint at $t = t_1$, the vehicles are in the asymmetric formation. At $t = t_2$, the formation becomes a line formation. Finally, at $t = t_3$ the last formation has the exact same separations as the original formation, but the positions of the real followers are swapped with the virtual followers'.

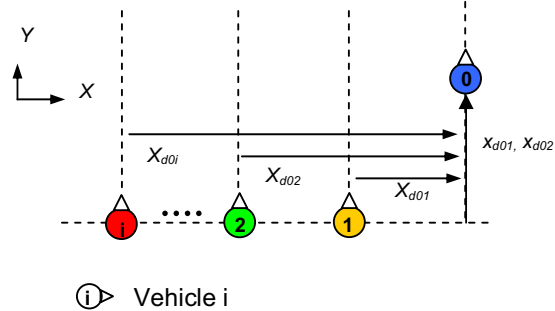


Fig. 4: Asymmetric Formation for Formation Swap Maneuver

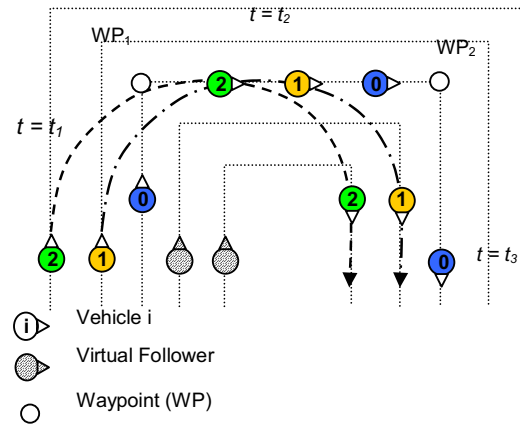


Fig. 5 : Formation Swap Maneuver

IV. SIMULATION RESULTS

The simulations were performed with three underwater vehicles with and without cross current disturbances. The waypoints were placed at every 20m to perform a lawn-mower search for the leader, and the followers are assigned to maintain a specified formation. The lateral distance of the formation given in Fig. 4 was defined with respect to the search field's coordinates. We set $X_{d01} = 45\text{m}$, $X_{d02} = 90\text{m}$, $X_{d0i} = 0\text{m}$, and $k = 10\text{m}$. A turning radius of the followers was chosen for k for an optimal 90deg turn. This formation shape minimizes search time and maximizes probability of detecting objects [14]. With this setup, the followers would always be chasing the point, and the formation shape will be the one given in Fig. 4 at steady state. The disturbance was defined as a random walk disturbance with the maximum magnitude of 1/5 of the vehicle's operating speed.

Fig. 6 shows the leader and the followers' heading responses. Only the responses for the first 180deg turn are considered, as the rest of them are merely repetition. It is interesting to see that the leader had 9% of overshoot while

the followers had a well-damped response. We also observe that the leader had more oscillation due to its effort to reach the waypoints. On the contrary, the followers did not have any oscillation once they were converged to the formation.

Fig. 7 and Fig. 8 show the convergence of the formation error in X and Y direction respectively. We observe that the followers took approximately 20sec to converge to the formation after each 90deg turn. Both followers had a steady state formation error of 1.2m in X-direction and 0.5m in Y-direction.

Fig. 9a and Fig. 9b show the trajectories of the vehicles. The rectangular region drawn by a solid line is a search field. When the formation swap was not used, the vehicles clearly spent a lot of time outside of the search area (Fig. 9a). In addition, the vehicles took more time to converge to the formation due to the significant difference in the lengths of the curvature. As a result, they had poor formation regulation and tracking performance. Moreover, the vehicles had to sweep every other lane because the platoon required a large turning radius. On the other hand, the formation swap allowed the vehicles to have similar turning radius, and the search was done efficiently (Fig. 9b). Most notably, the followers had much smaller tracking error with the formation swap maneuver. The multi-vehicle search performances were compared with a single-vehicle search in Table 1. The tracking errors within the search field were used to calculate the standard deviations. The multi-vehicle searches had a larger standard deviation of tracking error (σ_{tr}) than the single-vehicle search because the followers maintained distance to the leader, not to the search lanes. With the formation swap, the total search time was reduced by 50% compared to the single-vehicle search and by 37% compared to the multi-vehicle search without the formation swap.

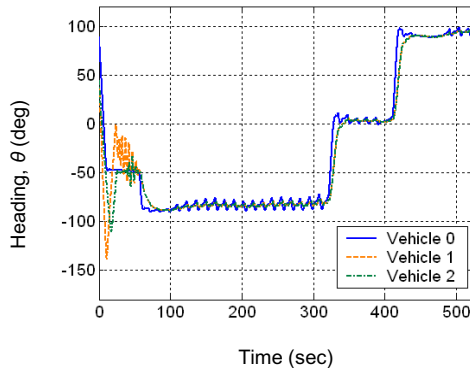


Fig. 6: Leader and Followers' Heading Response

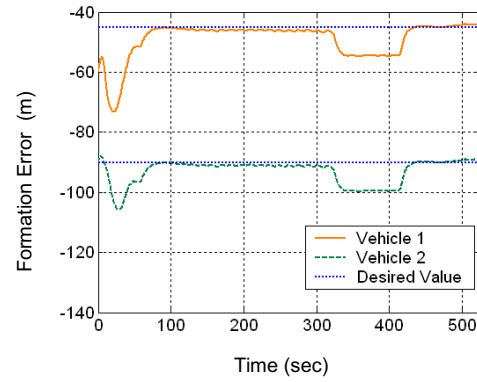


Fig. 7: Formation Error in X-direction

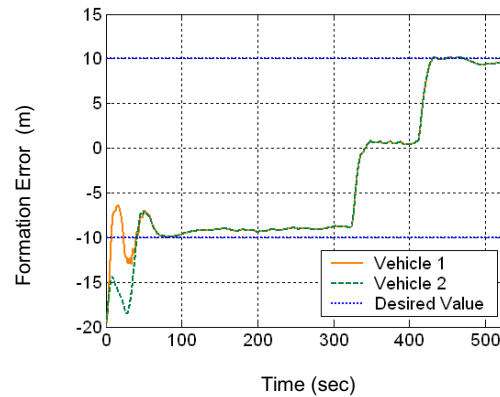


Fig. 8: Formation Error in Y-Direction

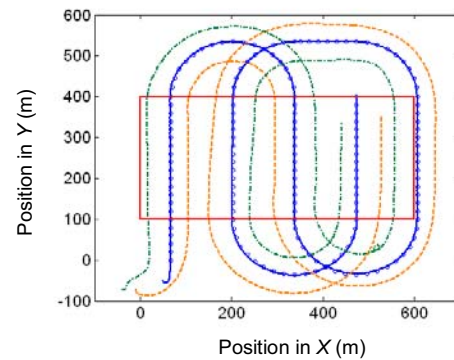


Fig 9a : Multi-vehicle Search without Formation Swap Maneuver
Solid: Vehicle 0, Dashed: Vehicle 1, Dash-dot: Vehicle 2

Table 1: Summary of Simulation Results

	Without Disturbances				With Disturbances			
	t_{total} (min)	Standard Deviation of Tracking Error, σ_{tr}			t_{total} (min)	Standard Deviation of Tracking Error, σ_{tr}		
		Vehicle 0	Vehicle 1	Vehicle 2		Vehicle 0	Vehicle 1	Vehicle 2
Single Vehicle Search	51.4	0.23	---	---	50.6	1.52	---	---
Multi-Vehicle Search	39.2	0.49	1.57	1.13	39.1	1.37	6.5	6.69
Multi-Vehicle Search (with Formation Swap)	24.9	0.18	0.56	0.49	24.6	1.05	2.49	1.79

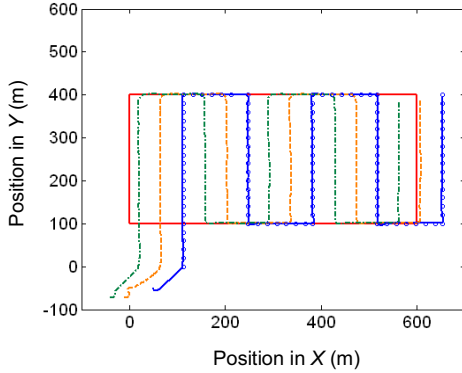


Fig. 9b: Multi-vehicle Search with Formation Swap Maneuver
Solid: Vehicle 0, Dashed: Vehicle 1, Dash-dot: Vehicle 2

VI. CONCLUSION

We presented the design of a robust multivariable controller for decentralized leader-follower control of a platoon of autonomous underwater vehicles. The leader used a waypoint guidance system, and followers used a similar guidance system and speed controller to the leader's to follow the leader. Linear Quadratic Gaussian regulator theory and Loop Transfer Recovery techniques were used to design the robust steering and the speed controller. The formation swap maneuver was introduced to make efficient 180deg turns with a platoon. The simulation results under a cross current disturbance showed the effectiveness of the controller.

ACKNOWLEDGMENT

The authors gratefully acknowledge the support of the Office of Naval Research, which has supported this work under the award "Decentralized Control of Multiple Autonomous Underwater Vehicles" No. N00014-03-1-0634.

REFERENCES

- [1] J. Doyle, and G. Stein, "Robustness with observers," *IEEE Trans. Automatic Control*, Vol. 24, 4, pp. 607-611, August 1979.
- [2] J. Doyle, and G. Stein, "Multivariable feedback design: Concepts for a classical/modern synthesis," *IEEE Trans. Automatic Control*, Vol. 26, 1, pp. 4-16, February 1981.
- [3] J.R. Edwards, "Bistatic Synthetic Aperture Target Detection and Imaging With an AUV," *IEEE J. Oceanic Engineering*, Vol. 26, 4, October 2001.

- [4] T.I. Fossen, *Guidance and Control of Ocean Vehicles*, John Wiley & Sons, Inc, August 1994.
- [5] A.J. Healey, and D. Lienard, "Multivariable sliding mode control for autonomous diving and steering of unmanned underwater vehicles," *IEEE J. Oceanic Engineering*, Vol. 18, 3, pp. 327-339, July 1993.
- [6] A.J. Healey, "Application of formation control for multi-vehicle robotic minesweeping," *Proc. the 40th IEEE Conf. Decision and Control*, Vol. 2, pp. 1497-1502, December 2001.
- [7] D.L. Juul, "Submersible Control Using the Linear Quadratic Gaussian with Loop Transfer Recovery Method," *Autonomous Underwater Vehicle Technology*, pp. 417-425, July 1994.
- [8] W. Kang, A. Sparks, and S. Banda, "Multi-satellite formation and reconfiguration," *American Control Conf.*, Vol. 1, 6, pp. 379 -383, June 2000.
- [9] Y. Kuroda, T. Ura, and K. Aramaki, "Vehicle Control Architecture for Operating Multiple Vehicles," *Autonomous Underwater Vehicle Technology*, pp. 323-329, July 1994.
- [10] F.L. Lewis, *Optimal Control*, John Wiley & Sons, Inc., 1995.
- [11] R.J. Martin, L. Valavani, M. Athans, "Multivariable Control of a Submersible Using the LQG/LTR Design Methodology," *Proc. American Control Conf.*, pp. 1313-1324, 1986.
- [12] M.J. Mataric, M. Nilsson, and K.T. Simsarin, "Cooperative multi-robot box-pushing," *Intelligent Robots and Systems 95, Human Robot Interaction and Cooperative Robots, Proc, 1995 IEEE/RSJ International Conf*, Vol. 3, pp. 556 -561, August 1995.
- [13] W. Naeem, R. Sutton and S.M. Ahmad, "LQG/LTR control of an autonomous underwater vehicle using a hybrid guidance law", *Proc. of GCUV'03 conf.*, pp. 35-40, April, 2003.
- [14] A. Okamoto, "Robust Control of a Platoon of Autonomous Underwater Vehicles," *M.S. Thesis*, University of Idaho, December 2003.
- [15] T. Prestero, "Verification of a six-degree of freedom simulation model for the REMUS autonomous underwater vehicle," *M.S. Thesis*, Massachusetts Institute of Technology and Woods Hole Oceanographic Institution, September 2001.